Revista Brasileira de Geofísica
RBGf
Brazilian Journal of Geophysics

Revista Brasileira de Geofísica (2012) 30(1): 41-49

ISSN 0102-261X
www.scielo.br/rbg

DETECTION OF LATERITIC DEPOSITS USING TM LANDSAT IMAGES IN ORDER TO SUPPORT THE CARAJÁS RAILWAY DUPLICATION PROJECT, NORTH AND NORTHEASTERN BRAZIL

Marcos Eduardo Hartwig[1] and Fábio di Giaimo Caboclo[2]

Recebido em 12 março, 2011 / Aceito em 2 janeiro, 2012
Received on March 12, 2011 / Accepted on January 2, 2012

ABSTRACT. The aim of this study was to map iron duricrust in order to subsidize the Carajás Railway duplication project, in a tract of approximately 200 km, located between the states of Pará and Maranhão, north and northeast regions of Brazil. The vegetation is constituted of crop areas and grassland. The methodology is based on the Crósta technique applied to six and four bands of the TM Landsat 5. The results showed that the application of the technique to four bands was more effective to detect iron oxides. In the center-north to northeast of the study area, where a wide dissected plateau occurs, potential iron oxide concentrations are observed, which are coincident with the main duricrust registered occurrences and roughly with the lateritic deposits located in the geological map.

Keywords: duricrust, TM Landsat, Crósta technique, construction material, Carajás Railway.

RESUMO. O objetivo deste trabalho foi mapear crostas lateríticas ferruginosas para subsidiar o projeto de duplicação da Ferrovia Carajás, num trecho de aproximadamente 200 km, constituído, principalmente, por áreas agrícolas e pastagens, localizado entre os estados do Pará e Maranhão, regiões Norte e Nordeste do Brasil. A metodologia enfocou a técnica Crósta, aplicada a seis e quatro bandas espectrais do sensor TM Landsat 5. Os resultados mostraram que a aplicação da técnica a quatro bandas foi mais eficiente na detecção de minerais de óxido de ferro. Nas regiões centro-norte e nordeste da área de estudo, caracterizadas por um amplo platô dissecado, encontram-se potenciais concentrações de minerais de óxido de ferro, que coincidem com as principais ocorrências cadastradas e aproximadamente com os depósitos lateríticos indicados no mapa geológico.

Palavras-chave: cobertura laterítica, TM Landsat, técnica Crósta, material de construção, Ferrovia Carajás.

[1]Planservi Engenharia Ltda., Avenida Professor Ascendino Reis, 725, Vila Clementino, 04027-000 São Paulo, SP, Brazil. Phone: +55 (12) 8212-9204 / 3208-6442 – E-mail: marcoshartwig@gmail.com

[2]Planservi Engenharia Ltda., Avenida Professor Ascendino Reis, 725, Vila Clementino, 04027-000 São Paulo, SP, Brazil. Phone/Fax: +55 (11) 3304-1481 – E-mail: fabio.caboclo@gmail.com

INTRODUCTION

The Carajás Railroad is situated in the north and northeast regions of Brazil, with approximately 1,000 km extension and connects the Carajás Iron Mine, on the southeast of the Pará State, to the Ponta da Madeira Port, in São Luís, Maranhão State. Due to the high consumption of iron ore during the last years, a project for duplication of the railroad is being developed. Due to the lack of materials with adequate geotechnical properties to be used as railroad sub-ballast, option was made, under others, to use ferruginous lateritic duricrust.

The lateritic duricrust coverage, according to Beauvais & Colin (1993) and Bigarella et al. (1996) would be the result of laterization processes – intense chemical weathering from any preexisting rock – in regions of tropical climate with long dry periods and an annual rainfall between 1,200 and 1,800 mm. In the Amazon Region they have a wide distribution and would have been formed during the Lower Tertiary and the Quaternary (Pleistocene), as a result of the action of the South American and Paraguaçu/Manzerini (Costa, 1991) peneplain surfaces.

The study area is located between the cities of Marabá, Pará State and Açailândia, Maranhão State, and includes part of the Carajás Railroad with approximately 200 km extension (Fig. 1). In this region, an ample dissected plateau occurs at north and northeast, with a maximum elevation of 475 m a.s.l., and ample hills and isolated hillocks appear at southwest. The original vegetation may be divided in open forest with "Cerrado" insets and dense forest, both extensively substituted by agriculture, and by pastures used to breed cattle. In the more outstanding portions of the relief, are found isolated remnants of ferruginous lateritic crust covers, developed over Cretaceous sandstones from Itapecuru Formation, which are being explored and used in civil engineering constructions.

The use of Landsat images for regional mineral exploration is being used, with success, by various researchers such as Kaufmann (1988), Varajão et al. (1988), Fraser (1991), Loughlin (1991), Bennett et al. (1993), Crósta & Rabelo (1993), Crósta & Souza Filho (2009), under others. In this sense, the purpose of this work is to determine the areas with best occurrence potential of ferruginous lateritic crusts, using the digital processing of TM images, in order to support future field surveys, which implies in time and resources savings. For that purpose the "Crósta technique" was used, known as a variation of the principal components transform (Crósta & Moore, 1989).

MATERIAL AND METHOD

In tropical regions the natural vegetation may dramatically limit the application of the multispectral sensor data, in minerals' detection and mapping, since it tarnishes their spectral answer (Siegal & Goetz, 1977; Carranza & Hale, 2002). Although the region under study is located on the periphery of the Amazon Region, where originally open forests and "Cerrado" insets and dense forests occurred (BRASIL, 1973; BRASIL, 1974), both were intensively substituted by agriculture and pastures for cattle breeding, which increases the possibilities for success in relation to the use of remote sensors in mineral surveys.

Considering this, the methodology was based on digital images from the TM Landsat 5, using applications Spring 5.1 and ArcGis 9.x. The area under study is covered by the scenes/point orbit 222/63, 222/64, 223/63 and 223/64, obtained in different dates during the dry season. The satellite images are freely available at: <http://www.cbers.inpe.br/>. In this work the Geographic Coordinate System and Datum SAD69 were used.

The original images were not submitted to any pre-processing, with exception of the geometric correction, as demonstrated by Loughlin (1991). The image processing focused on the reflectance in the 350-1,500 nm interval of the electromagnetic spectrum, associated to the minerals of the iron oxide group (Fig. 2, Hunt & Salisbury, 1970). The "Crósta technique" was individually applied to the set of images of each scene (Crósta & Moore, 1989), a variation of the principal components transform, which aims to remove the information redundancy contained in the original images. In a simplified view, it is based on the previous knowledge of the spectral signature of specific targets in the spectral bands, in order to define and select the principal components which contain the desired information. An important aspect of this technique is that it indicates, based on the signal and magnitude contributions of each original image, if the target of interest will be enhanced in the PCs images as light pixels (high digital levels) or dark (low digital levels). This successful technique is being used by many researchers (Loughlin, 1991; Crósta & Rabelo, 1993; Davidson et al., 1993; Ruiz-Armenta & Prol-Ledesma, 1998; Souza Filho & Drury, 1998; Sabine, 1999; Carranza & Hale, 2002; Tagestani & Moore, 2002; Ranjbar et al., 2004).

STUDY AREA

Geology

The study area (Fig. 1) includes lithotypes from the Amazon Craton, Tocantins Province and Parnaíba Province, varying in ages from the Mesoarchean to the Cretaceous (Faraco et al., 2004; Vasconcelos et al., 2004).

The Amazon Craton is represented by charnockitoids, included in the Cajazeiras Enderbite unit, which crops out exclusively in the northeast portion of the area.

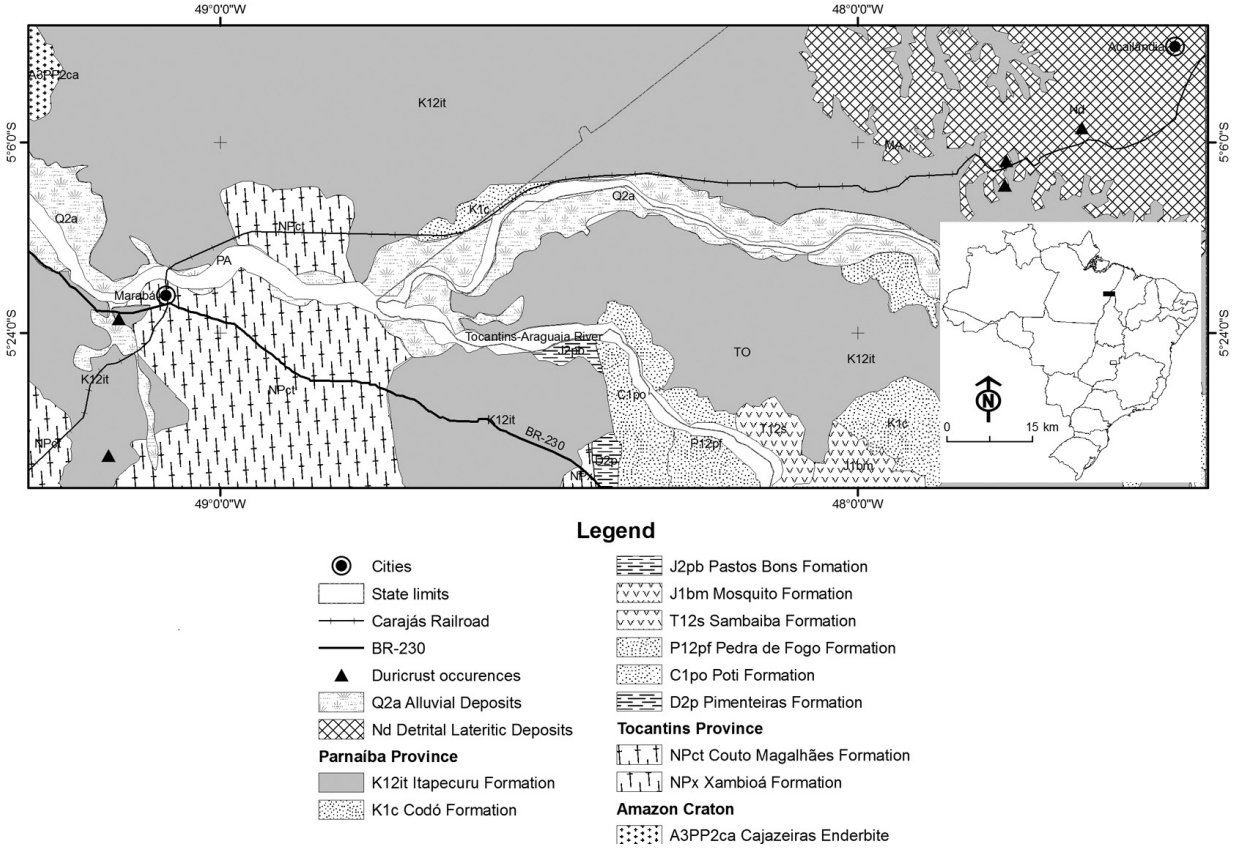

Figure 1 – Geologic map of the study area based on Faraco et al. (2004) and Vasconcelos et al. (2004).

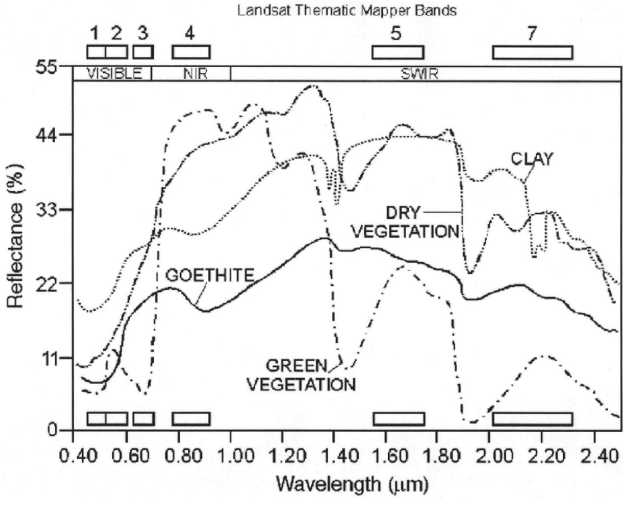

Figure 2 – Spectral signatures of iron oxide, vegetation and clay. Extracted from Carranza & Hale, 2002.

The units included in the Tocantins Province crop out in the center-west region, and are constituted by very weathered rocks, represented by phyllites, shales and slates, with an approximate N-S orientation, belonging to Couto Magalhães and Xambioá Formations.

The Parnaíba Province covers the largest portion of the study area and includes, mostly, transitional and marine fluvial sandstones, of Devonian and Cretaceous age, included in Itapecuru, Codó, Pastos Bons, Pedra do Fogo, Poti and Pimenteiras Formations, besides igneous bodies of basic and alkaline igneous

bodies, cropping out in the extreme south (Mosquito and Sambaiba Formations). Under the outcropping units are the fluvial sandstones and pelites from Itapecuru Formation which are the most important expression in the area. Over this unit is described a detrital/lateritic coverage with Tertiary age.

Quaternary sediments crop out along the Tocantins and Araguaia River plains and their main tributaries, being constituted by unconsolidated sands, clays and gravel levels.

Lateritic coverage

The lateritic coverage, according to Beauvais & Colin (1993) and Bigarella et al. (1996) may be classified in two distinct types: *autochthonous* and *allochthonous*. The autochthonous, which are of special interest for this work, are conformed by an upper duricrust or concretionary horizon mainly constituted by minerals such as hematite and goethite.

The lateritic coverage occupies the top and middle slope portions. The duricrust horizon is a lithified layer of red color and nodular, columnar or, more rarely planar structure, with thicknesses in the order of 0.5-3 m, which vertically turns into reddish and yellowish latosols (Figs. 3, 4, 5). The organic horizon, if present, has a thickness of less than 0.5 m.

Figure 3 – Lateritic coverage with columnar structure. Thickness in the order of 2.5 m. Fazenda Água Boa, Cidelândia, Maranhão State.

Figure 4 – Detail of the duricrust horizon in the middle of the lateritic profile. Note the abundance of lithorelicts. Highway BR-230, Km 05.

IMAGE ANALYSIS AND PROCESSING

The geologic remote sensing must consider, not only the geologic model of the specific targets, but also the typology, occurrence and spectral characteristic of the other materials which constitute the landscape (for example, relief, hydrography, vegetation, soil use), since they contribute to the spectral answer of each pixel, and help in the data interpretation.

The colored composition R5G4B3 (Fig. 6) enhances those aspects of the landscape. Based on the method adopted in this work, the most propitious areas for the identification of the lateritic coverage would by those where the vegetation cover is absent or incipient. Those areas are generally (pink color), concentrated in the north-northeast, center-south and southeast regions.

Crósta technique applied to six spectral bands

Tables 1, 2, 3 and 4 provide the matrices of the eigenvectors from the principal components transform applied to the six original TM bands reflected from scenes/point orbit 222/63, 222/64, 223/63 and 223/64, which cover the study area. The PC1 of Table 1 does not indicate a significant spectral feature, since it is composed by a positive mixture of all bands, in this case with a higher proportion of band TM5, showing information about topography (shading) and albedo. The magnitude of the eigenvalues indicates that more than 90% of the information of the images of the PCs is contained in this principal component. The PC2 is dominated by the contribution of TM4, which presents the spectral answer due to vegetation. The PC3 demonstrates the contrast between the spectral information of the visible (channels 1-2-3) and of the infrared from the electromagnetic spectrum (channels 4-5-7).

Figure 5 – Occurrence of boulders in the duricrust horizon. Coordinates: Lat/Long 5°29′36,09″S/49°11′59,55″W.

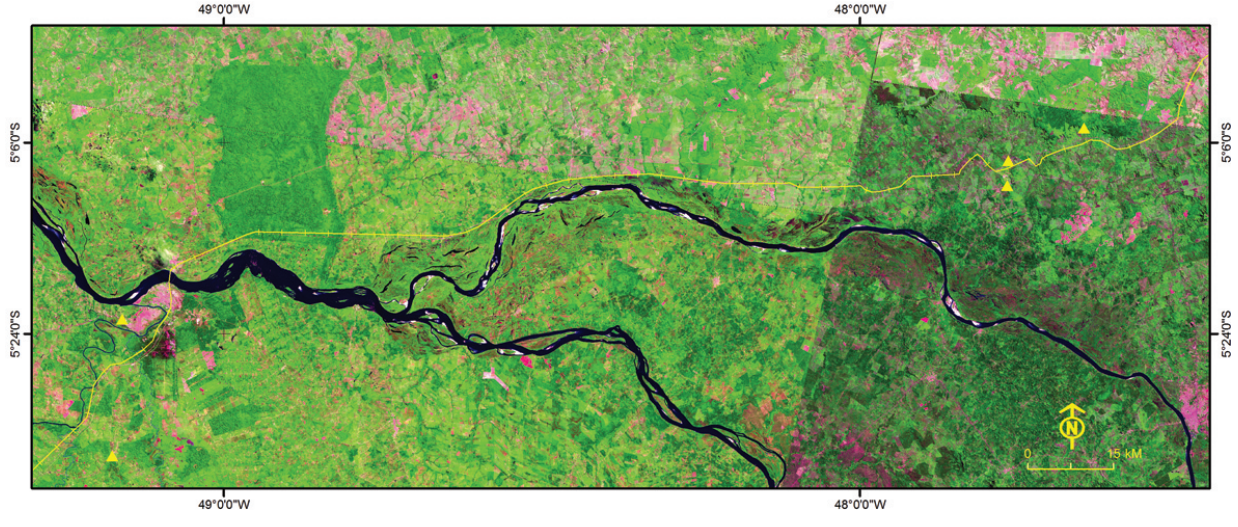

Figure 6 – Color composition R5G4B3. The green color indicates vegetation (undifferentiated), the pink, is exposed soil and the magenta indicates urban areas. The continuous yellow line represents the approximate position of the Carajás Railroad. The yellow triangles correspond to the occurrence of catalogued lateritic crusts.

Since the three first PCs do not show any information about the iron oxide minerals, the three other will contain the spectral information referring to these minerals. It should be mentioned that the information of interest represents only 0.14% of the total variance of the scene. The PC4 is formed through moderate contributions and opposed signals of the TM1 (23.44%), TM2

(−35.41%) and TM3 (−12.92%) bands. Since the iron oxide minerals have absorption in the TM1 and TM2 bands and high reflectance in TM3 band, they will be enhanced as dark pixels in PC4. The PC4 also presents a moderate negative contribution from TM4 (−12.44%), which indicates that the vegetation will also be enhanced as dark pixels. PC5 is formed by moderate to high contributions and opposed signals of TM5 (−18.99%) and TM7 (49.72%) bands. In nature, the clay minerals are one of the most common products deriving from rock weathering. In accordance with Figure 2, they exhibit high reflectance in TM5 band and little absorption in TM7 band. Thus, the clay minerals are mapped as dark pixels in PC5. In PC6 the iron oxide minerals are mapped as light pixels, since there is an intense reflection in TM4 band (50.88%) and low to moderate absorption in TM1 (−8.77%) and TM2 (−25.73%) bands.

Table 1 – Matrix of eigenvectors from the six original TM bands reflected from the scene/point orbit 222/63. The cells enhanced in bold indicate the PCs which contain spectral information referring to iron oxide minerals.

	TM1	TM2	TM3	TM4	TM5	TM7	Eigenvalue (%)
PC1	0.49 21.59%	0.23 10.13%	0.23 10.13%	0.51 22.47%	0.59 25.99%	0.22 9.69%	96.31
PC2	–0.12 –5.91%	0.28 13.79%	0.06 2.96%	–0.74 –36.45%	0.47 23.15%	0.36 17.73%	3.35
PC3	–0.70 –32.56%	–0.32 –14.88%	–0.24 –11.16%	0.32 14.88%	0.50 23.26%	0.07 3.26%	0.19
PC4	**0.49** **23.44%**	**–0.74** **–35.41%**	**–0.27** **–12.92%**	–0.26 –12.44%	0.25 11.96%	–0.08 –3.83%	0.09
PC5	0.05 2.79%	–0.14 –7.82%	–0.24 –13.41%	0.13 7.26%	–0.34 –18.99%	0.89 49.72%	0.04
PC6	**–0.15** **–8.77%**	**–0.44** **–25.73%**	**0.87** **50.88%**	–0.04 –2.34%	–0.06 –3.51%	0.15 8.77%	0.01

Table 2 – Matrix of eigenvectors from the six original TM bands reflected from the scene/point orbit 222/64. The cells enhanced in bold indicate the PCs which contain spectral information referring to iron oxide minerals.

	TM1	TM2	TM3	TM4	TM5	TM7	Eigenvalue (%)
PC1	0.54 24.22%	0.20 8.97%	0.23 10.31%	0.55 24.66%	0.53 23.77%	0.18 8.07%	95.27
PC2	–0.11 –5.42%	0.27 13.30%	0.04 1.97%	–0.67 –33.00%	0.56 27.59%	0.38 18.72%	3.11
PC3	0.73 35.10%	0.18 8.65%	0.22 10.58%	–0.44 –21.15%	–0.43 –20.67%	–0.08 –3.85%	1.29
PC4	**–0.34** **–14.91%**	**0.70** **30.70%**	**0.32** **14.04%**	0.21 9.21%	–0.39 –17.11%	0.32 14.04%	0.23
PC5	0.16 8.12%	–0.33 –16.75%	–0.31 –15.74%	0.08 4.06%	–0.26 –13.20%	0.83 42.13%	0.08
PC6	**–0.15** **–8.88%**	**–0.51** **–30.18%**	**0.83** **49.11%**	–0.05 –2.96%	–0.01 –0.59%	0.14 8.28%	0.02

The same reasoning may be extended to the eigenvectors matrices of Tables 2, 3 and 4, in which are exposed the statistical results of the principal components transform, applied to the six original bands of the other scenes. In these tables, PC1 may be interpreted as albedo and shading, PC2 represents the difference between the spectral bands of the visible and the infrared and PC3 maps vegetation. The spectral information referring to the iron oxide minerals is contained in the other PCs and corresponds to 0.9% of the total variance of the scenes. Thus, iron oxide minerals will be mapped as light pixels in PC4 and PC6 on Table 2, and the clay minerals will be mapped as dark pixels in PC5 and secondarily in PC4. In Table 3, the iron oxide minerals are mapped as light pixels in PC4 and as dark pixels in PC6, and the clay minerals mapped as dark pixels in PC5. In Table 4, the iron oxide minerals are mapped as light pixels in PC4 and as dark pixels in PC6 and the clay minerals are mapped as dark pixels in PC5 and PC4.

Table 3 – Matrix of eigenvectors from the six original TM bands reflected from the scene/point orbit 223/63. The cells enhanced in bold indicate the PCs which contain spectral information referring to iron oxide minerals.

	TM1	TM2	TM3	TM4	TM5	TM7	Eigenvalue (%)
PC1	0.50 22.32%	0.22 9.82%	0.21 9.38%	0.55 24.55%	0.56 25.00%	0.20 8.93%	96.16
PC2	–0.13 –6.47%	0.04 1.99%	0.23 11.44%	–0.69 –34.33%	0.56 27.86%	0.36 17.91%	3.41
PC3	0.76 37.25%	0.20 9.80%	0.20 9.80%	–0.42 –20.59%	–0.39 –19.12%	–0.07 –3.43%	0.30
PC4	**–0.36** **–17.31%**	**0.37** **17.79%**	**0.77** **37.02%**	0.16 7.69%	–0.31 –14.90%	0.11 5.29%	0.09
PC5	0.07 3.89%	–0.27 –15.00%	–0.12 –6.67%	0.12 6.67%	–0.34 –18.89%	0.88 48.89%	0.04
PC6	**–0.13** **–7.43%**	**0.83** **47.43%**	**–0.50** **–28.57%**	–0.05 –2.86%	–0.06 –3.43%	0.18 10.29%	0.01

Table 4 – Matrix of eigenvectors from the six original TM bands reflected from the scene/point orbit 223/64. The cells enhanced in bold indicate the PCs which contain spectral information referring to iron oxide minerals.

	TM1	TM2	TM3	TM4	TM5	TM7	Eigenvalue (%)
PC1	0.41 18.64%	0.20 9.09%	0.18 8.18%	0.60 27.27%	0.60 27.27%	0.21 9.55%	91.17
PC2	–0.04 –2.03%	0.06 3.05%	0.25 12.69%	–0.71 –36.04%	0.51 25.89%	0.40 20.30%	5.70
PC3	0.77 36.67%	0.31 14.76%	0.25 11.90%	–0.27 –12.86%	–0.40 –19.05%	–0.10 –4.76%	2.70
PC4	**–0.37** **–16.30%**	0.22 9.69%	**0.66** **29.07%**	0.22 9.69%	–0.39 –17.18%	0.41 18.06%	0.31
PC5	0.24 11.54%	–0.33 –15.87%	–0.41 –19.71%	0.06 2.88%	–0.27 –12.98%	0.77 37.02%	0.10
PC6	**–0.18** **–10.53%**	**0.84** **49.12%**	**–0.49** **–28.65%**	–0.03 –1.75%	–0.02 –1.17%	0.15 8.77%	0.02

If the number of spectral bands is reduced in the principal components transform, in order to avoid a certain spectral answer, the chances to concentrate the spectral answer of a certain mineral class in only one principal component increase (Loughlin, 1991). In this sense, as deduced from Figure 2, the principal components transform was applied to channels TM 1-3-4-5. The substitution of TM7 band by TM5 band produces a despicable effect in the analysis result. The omission of one infrared band has the purpose to avoid mapping of clay minerals.

Crósta technique applied to four spectral bands

The Tables 5, 6, 7 and 8 show the eigenvector matrices from principal components transform, applied to TM 1-3-4-5 bands from scenes/point orbit 222/63, 222/64, 223/63 and 223/64, which cover the study area. In them, PC1 may be interpreted as albedo and shading, since there is a positive contribution of all spectral bands, PC2 as vegetation, since it presents a high negative contribution to TM4 band and PC3 represents the difference between the visible (TM1-3) and the infrared (TM4-5) spectral bands.

Table 5 – Matrix of eigenvectors from TM 1-3-4-5 bands from the scene/point orbit 222/63, for the mapping of the iron oxide minerals. The cells enhanced in bold indicate the PC which contain spectral information referring to iron oxide minerals.

	TM1	TM3	TM4	TM5	Eigenvalue (%)
PC1	0.52 26.94%	0.25 12.95%	0.54 27.98%	0.62 32.12%	96.49
PC2	–0.07 –4.09%	0.33 19.30%	–0.74 –43.27%	0.57 33.33%	3.21
PC3	0.77 41.62%	0.29 15.68%	–0.31 –16.76%	–0.48 –25.95%	0.20
PC4	**–0.38** **–22.09%**	**0.86** **50.00%**	0.24 13.95%	–0.24 –13.95%	0.10

Table 6 – Matrix of eigenvectors from TM 1-3-4-5 bands from the scene/point orbit 222/64, for the mapping of the iron oxide minerals. The cells enhanced in bold indicate the PC which contain spectral information referring to iron oxide minerals.

	TM1	TM3	TM4	TM5	Eigenvalue (%)
PC1	0.56 29.47%	0.21 11.05%	0.58 30.53%	0.55 28.95%	95.57
PC2	–0.05 –2.94%	0.30 17.65%	–0.69 –40.59%	0.66 38.82%	2.91
PC3	0.78 43.33%	0.18 10.00%	–0.40 –22.22%	–0.44 –24.44%	1.33
PC4	**–0.26** **–16.25%**	**0.91** **56.88%**	0.17 10.63%	–0.26 –16.25%	0.20

Table 7 – Matrix of eigenvectors from TM 1-3-4-5 bands from the scene/point orbit 223/63, for the mapping of the iron oxide minerals. The cells enhanced in bold indicate the PC which contain spectral information referring to iron oxide minerals.

	TM1	TM3	TM4	TM5	Eigenvalue (%)
PC1	0.52 27.23%	0.22 11.52%	0.58 30.37%	0.59 30.89%	96.38
PC2	–0.09 –5.26%	0.27 15.79%	–0.69 –40.35%	0.66 38.60%	3.23
PC3	0.81 45.25%	0.18 10.06%	–0.41 –22.91%	–0.39 –21.79%	0.31
PC4	**–0.26** **–16.35%**	**0.92** **57.86%**	0.15 9.43%	–0.26 –16.35%	0.08

Table 8 – Matrix of eigenvectors from TM 1-3-4-5 bands from the scene/point orbit 223/64, for the mapping of the iron oxide minerals. The cells enhanced in bold indicate the PC which contain spectral information referring to iron oxide minerals.

	TM1	TM3	TM4	TM5	Eigenvalue (%)
PC1	0.43 22.99%	0.19 10.16%	0.63 33.69%	0.62 33.16%	91.90
PC2	0.03 1.79%	0.30 17.86%	–0.72 –42.86%	0.63 37.50%	5.19
PC3	0.84 48.28%	0.25 14.37%	–0.23 –13.22%	–0.42 –24.14%	2.65
PC4	**–0.33** **–20.50%**	**0.90** **55.90%**	0.17 10.56%	–0.21 –13.04%	0.26

The spectral information referring to the iron oxide minerals is contained in PC4, which corresponds to only 0.64% of the total variance of the scenes. In Table 5 the iron oxide minerals are mapped as light pixels, since they present high contributions of opposed signals in TM1 (-22,09%) and TM3 (50%) bands. In analog form, in Tables 6, 7 and 8 the iron oxide minerals are mapped in PC4 as light pixels. Figure 7 depicts the mosaic of images from PC4 from the different scenes, in which the iron oxide minerals are enhanced as light regions. It can be noticed that the concentrations are constituted by little fragmented areas, mostly concentrated in the north-northeast portion, which coincides with an ample dissected plateau and to areas with exposed soil, where the largest and thickest occurrences of lateritic crusts were determined. The results are also approximately coincident with what is indicated in the regional geologic map (Fig. 1).

CONCLUSION

The results obtained allow to conclude that:

- The application of the Crósta technique with four spectral bands has proven to be more efficient for the mapping of the iron oxide minerals.

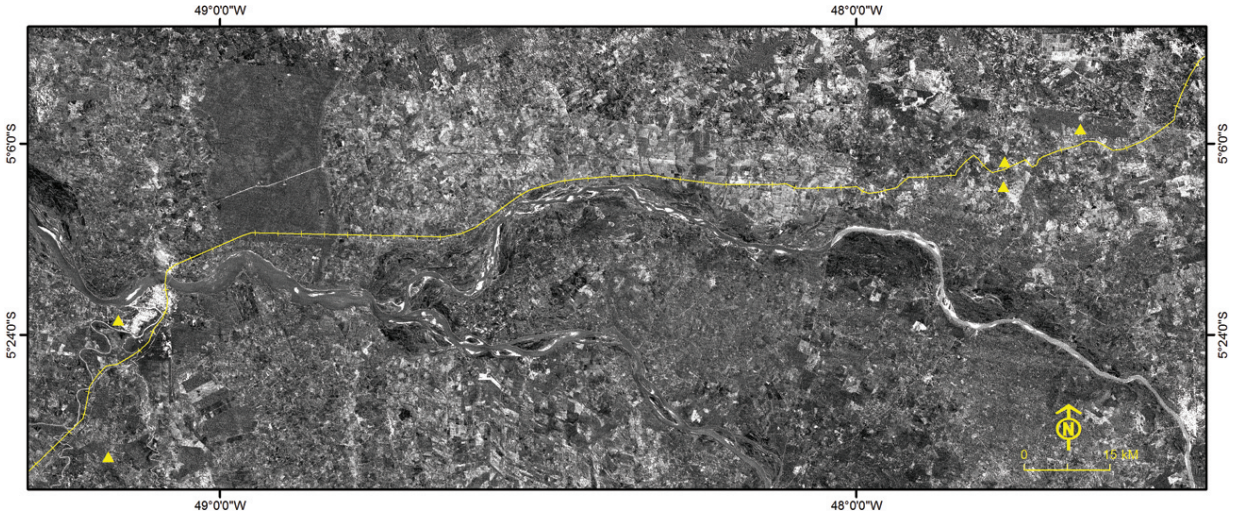

Figure 7 – Mosaic of images from PC4 from the scenes/point orbit 222/63, 222/64, 223/63 and 223/64, generated from the principal components transform of the original TM 1-3-4-5 channels. The iron oxide minerals are enhanced as light regions. The continuous yellow line represents to the approximate position of the Carajás railroad. The yellow triangles correspond to known occurrences.

- The PC 4 contains the spectral information referring to the iron oxide minerals in the study area. It can be noticed that the concentrations are constituted by little fragmented areas, which occur, mostly, in the north-northeast portion. These areas coincide with an extended dissected plateau and of areas with exposed soil, where the largest and thickest occurrences of lateritic crusts were determined. The results also coincide approximately with the information of the geologic map.
- The concentrations of iron oxide minerals indicate the geographic proximity with the railroad track, and so they become potential targets to be investigated.

ACKNOWLEDGMENTS

The authors would like to express their sincere acknowledgments to Professors Álvaro Crósta from IG-Unicamp and Carlos Tadeu de Carvalho Gamba from SENAC/Sto. Amaro for reading the manuscript.

REFERENCES

BEAUVAIS A & COLIN F. 1993. Formation and transformation processes of iron duricrust systems in tropical humid environment. Chem. Geol., 106: 77–101.

BENNETT SA, ATKINSON WW & KRUSE FA. 1993. Use of Thematic Mapper imagery to identify mineralization in the Santa Teresa district, Sonora, Mexico. International Geology Review, 35: 1009–1029.

BIGARELLA JJ, BECKER RD & PASSOS E. 1996. Estrutura e origem das paisagens tropicais e subtropicais. Florianópolis: Editora da UFSC, vol. II. p. 566–612.

BRASIL. 1973. Ministério de Minas e Energia. Departamento Nacional de Produção Mineral. Projeto RADAMBRASIL Folha SB.23 Teresina e parte da Folha SB.24 Jaguaribe. Rio de Janeiro (Levantamento de Recursos Naturais, 2).

BRASIL. 1974. Ministério de Minas e Energia. Departamento Nacional de Produção Mineral. Projeto RADAMBRASIL Folha SB.22 Araguaia e parte da Folha SC.22 Tocantins. Rio de Janeiro (Levantamento de Recursos Naturais, 4).

CARRANZA EJM & HALE M. 2002. Mineral imaging with Landsat Thematic Mapper data for hydrothermal alteration mapping in heavily vegetated terrain. International Journal of Remote Sensing, 23: 4827–4852.

COSTA ML. 1991. Aspectos geológicos dos lateritos da Amazônia. Revista Brasileira de Geociências, 21(2): 146–160.

CRÓSTA A & MOORE JM. 1989. Enhancement of Landsat Thematic Mapper imagery for residual soil mapping in SW Minas Gerais State, Brazil: a prospecting case history in Greenstone belt terrain. In: Proceedings of the Seventh thematic conference on Remote Sensing for Exploration Geology. Proceedings, ERIM, Calgary, p. 1173–1187.

CRÓSTA AO & RABELO A. 1993. Assessing Landsat TM for hydrothermal mapping in central-western Brazil. In: Proceedings of the Ninth Thematic Conference on Geologic Remote Sensing, Pasadena, California, USA, 1053–1061.

CRÓSTA AP & SOUZA FILHO CR. 2009. Mineral exploration with Landsat Thematic Mapper (TM)/Enhanced Thematic Mapper Plus (ETM+): a

review of the fundamentals, characteristics, data processing and case studies. In: BEDELL R, CRÓSTA AP & GRUNSKY E (Eds.). Remote Sensing and Spectral Geology, 16: 59–82.

DAVIDSON D, BRUCE B & JONES D. 1993. Operational remote sensing mineral exploration in a semi-arid environment: the Troodos Massif. Cyprus. In: Thematic Conference on Geologic Remote Sensing. 9th. Pasadena. California. Environmental Research Institute of Michigan. Proceedings, 2: 845–859.

FARACO MTL, MARINHO PAC, VALE AG, COSTA EJS, MAIA RGN, FERREIRA AL, VALENTE CR, LACERDA FILHO JV, MORETON LC, CAMARGO MA, VASCONCELOS AM, OLIVEIRA M, OLIVEIRA IWB, ABREU FILHO WA & GOMES IP. 2004. Folha SB.22-Araguaia. In: SCHOBBENHAUS C, GONÇALVES JH, SANTOS JOS, ABRAM MB, LEÃO NETO R, MATOS GMM, VIDOTTI RM, RAMOS MAB & JESUS JDA de. (Eds.). Carta Geológica do Brasil ao Milionésimo, Sistema de Informações Geográficas. Programa Geologia do Brasil. CPRM, Brasília. CD-ROM.

FRASER SJ. 1991. Discrimination and identification of ferric oxides using satellite Thematic Mapper data: A Newman case study. International Journal of Remote Sensing, 12: 635–641.

HUNT GR & SALISBURY JW. 1970. Visible and near-infrared spectra of minerals and rocks: III oxides and hydroxides. Modern Geology, 2: 195–205.

KAUFMANN H. 1988. Mineral exploration along the Aqaba-Levant structure by use of TM-data: concepts, processing and results. International Journal of Remote Sensing, 9: 1639–1658.

LOUGHLIN WP. 1991. Principal component analysis for alteration mapping. Photogrammetric Engineering and Remote Sensing, 57: 1163–1170.

RANJBAR H, HONARMAND M & MOEZIFAR Z. 2004. Application of the Crósta technique for porphyry copper alteration mapping using ETM+ data in the southern part of the Iranian volcanic sedimentary belt. Journal of Asian Earth Sciences, 24: 237–243.

RUIZ-ARMENTA JR & PROL-LEDESMA RM. 1998. Techniques for enhancing the spectral response of hydrothermal alteration minerals in Thematic Mapper images of Central Mexico. International Journal of Remote Sensing, 19: 1981–2000.

SABINE C. 1999. Remote Sensing Strategies for Mineral Exploration. In: RENCZ AN (Ed.). Remote Sensing for the Earth Sciences – Manual of Remote Sensing. New York: John Wiley and Sons, Inc., 3rd ed., 3: 375–447.

SIEGAL BS & GOETZ AFH. 1977. Effect of vegetation on rock and soil type discrimination. Photogrammetric Engineering and Remote Sensing, 42(2): 191–196.

SOUZA FILHO CR & DRURY SA. 1998. Evaluation of JERS-1 (FUYO-1) OPS and Landsat TM images for mapping of gneissic rocks in arid areas. International Journal of Remote Sensing, 19: 3569–3594.

TAGESTANI MH & MOORE F. 2002. Porphyry copper alteration mapping at the Meiduk area, Iran. International Journal of Remote Sensing, 23(22): 4815–4825.

VARAJÃO CAC, MENESES PR, CARVALHO A, MELFI AJ & BOULANGÉ B. 1988. Detecção de depósitos bauxíticos em coberturas lateríticas através de imagens TM, sinclinal do Gandarela, Quadrilátero Ferrífero, MG. V Simpósio Brasileiro de Sensoriamento Remoto, Natal, RN. Anais, 2: 275–281.

VASCONCELOS AM, RIBEIRO JAP, COLARES JQS, GOMES IP, FORGIARINI LL & MEDEIROS MF. 2004. Folha Teresina SB.23. In: SCHOBBENHAUS C, GONÇALVES JH, SANTOS JOS, ABRAM MB, LEÃO NETO R, MATOS GMM, VIDOTTI RM, RAMOS MAB & JESUS JDA de. (Eds.). Carta Geológica do Brasil ao Milionésimo, Sistema de Informações Geográficas. Programa Geologia do Brasil. CPRM, Brasília. CD-ROM.

NOTES ABOUT THE AUTHORS

Marcos Eduardo Hartwig. Graduated in Geology at Universidade Estadual Paulista (Unesp, 2003), M.Sc. in Geosciences at Universidade de São Paulo (USP, 2006) and specialization in geoprocessing at Serviço Nacional de Aprendizagem Comercial (Senac, 2010). Acted as engineering geologist in infrastructure projects in Brazil and abroad. Presently develops a Ph.D. project at the Instituto Nacional de Pesquisas Espaciais (INPE). Areas of interest in geological remote sensing and engineering geology.

Fábio di Giaimo Caboclo. Graduated in Civil Engineering at Universidade de São Paulo (USP, 1993), post-graduate in Business Administration at Fundação Getúlio Vargas (FGV, 1997) and MBA in Finances at Instituto Brasileiro de Mercado de Capitais (IBMEC, 2002). Presently acts as coordinator of engineering infrastructure projects in Brazil and abroad. Research interest in new management tools applied to engineering.